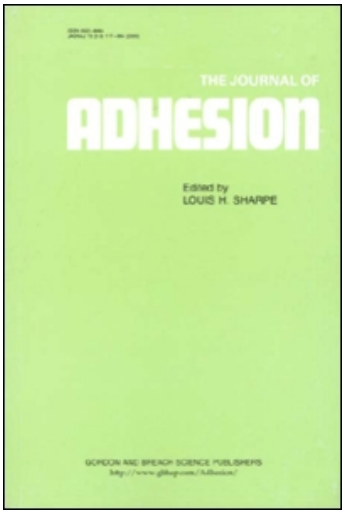

The Journal of Adhesion
Publication details, including instructions for authors and subscription information:
http://www.informaworld.com/smpp/title~content=t713453635

ANALYTICAL SOLUTIONS FOR PEELING USING BEAM-ON-FOUNDATION MODEL AND COHESIVE ZONE

Raymond H. Plaut[a]; Jennifer L. Ritchie[a]
[a] Center for Adhesive and Sealant Science, Blacksburg, Virginia, USA

Online publication date: 10 August 2010

To cite this Article Plaut, Raymond H. and Ritchie, Jennifer L.(2004) 'ANALYTICAL SOLUTIONS FOR PEELING USING BEAM-ON-FOUNDATION MODEL AND COHESIVE ZONE', The Journal of Adhesion, 80: 4, 313 — 331
To link to this Article: DOI: 10.1080/00218460490445832
URL: http://dx.doi.org/10.1080/00218460490445832

The Journal of Adhesion, 80: 313–331, 2004

ISSN: 0021-8464 print/1545-5823 online
DOI: 10.1080/00218460490445832

Taylor & Francis
Taylor & Francis Group

ANALYTICAL SOLUTIONS FOR PEELING USING BEAM-ON-FOUNDATION MODEL AND COHESIVE ZONE

Raymond H. Plaut
Jennifer L. Ritchie
Center for Adhesive and Sealant Science, Virginia Polytechnic Institute and State University, Blacksburg, Virginia, USA

When fibrillation occurs during peeling, the normal stress in the adhesive may gradually reduce to zero at the peel front. The shear stress also reduces to zero. Classical beam-spring (or beam-on-elastic-foundation) models do not yield solutions that have these properties. With the use of a beam-on-foundation model combined with a cohesive zone in the neighborhood of the peel front, these properties can be satisfied. In order to obtain analytical solutions, peel tests are considered in which the backing has a small slope and is linearly elastic in the adhered region, and the traction law is assumed to be piecewise linear. Cases are considered with only normal stresses in the adhesive (mode I), only shear stresses (mode II), and both stresses coupled (mixed-mode behavior). Analytical solutions are obtained for displacements of the backing, forces in the backing, and stresses between the adhesive and the backing.

Keywords: Cohesive zone models; Elastic peel arm; Elastic–plastic foundation; Piecewise–linear models; Peel test

INTRODUCTION

In a standard peel test, a tape consisting of a backing and an adhesive is peeled from a flat rigid surface. The shear stress in the adhesive must reduce to zero at the peel front. In addition, if fibrillation occurs in the neighborhood of the peel front, the normal force in the adhesive also may gradually reduce to zero at the peel front, as shown by

Received 20 August 2003; in final form 13 February 2004.
This research was supported by the National Science Foundation under Grant No. CMS-9713949. The authors are grateful to the reviewers for their helpful comments.
Address correspondence to Raymond H. Plaut, Department of Civil and Environmental Engineering, Virginia Tech, Mail Code 0105, Blacksburg, VA 24061, USA. E-mail: rplaut@vt.edu

experimental results [1]. A classical formulation of the peel test assumes that the backing is an elastic beam and that the adhesive acts as an elastic foundation (*i.e.*, as a distribution of normal and shear springs). If the slope of the attached tape is small, the formulation is often reduced to uncoupled linear differential equations for the normal and shear stresses, and analytical solutions can be obtained [2].

In the analysis of lap joints, Wang *et al.* [3] superposed an elastic foundation solution with another function so that the shear stress at the end of the adhesive is reduced to zero. Continuum models for lap joints that use the zero-shear-stress boundary condition include those in Allman [4] Chen and Cheng [5], and Adams and Mallick [6]. Yang *et al.* [7, 8] applied a "trapezoidal" cohesive zone model to examine normal and shear stresses in the fracture of adhesively bonded joints, and mixed-mode cases were discussed by Thouless and Yang [9].

For the analysis of peel tests, such trapezoidal cohesive zone models were utilized by Wei and Hutchinson [10] and Yang *et al*. [11]. The traction–separation relationship was assumed to be piecewise linear, with a positive slope at first (elastic behavior), then a constant slope (perfectly plastic behavior), and then a negative slope (called "damage" in Williams and Hadavinia [12]) till the stress decreased to zero. This type of behavior approximates that which is sometimes seen in experimental results involving fibrillation in probe tests [13, 14] as well as peel tests [1]. Some analytical solutions related to peeling and a cohesive zone were presented in Yamada [15] and recently in Williams and Hadavinia [12] and Georgiou *et al.* [16]. Shear of the adhesive was not considered, and the traction law for the normal stress included one or two linear sections. The analyses of Williams and Hadavinia [12], Yamada [15], and Georgiou *et al.* [16] are generalized here. (Another study involving peeling and a cohesive zone is Rahulkumar *et al.* [17], and Cotterell *et al.* [18] have organized a "round robin" to compare results of inelastic beam models and cohesive zone finite element analyses.)

In this article the basic formulation is described in the next section, and the trapezoidal traction law used in Yang *et al*. [7, 8, 11], Yang and Thouless [9], and Wei and Hutchinson [10] is applied for the case of negligible shear stress in the adhesive (mode I) in the following section. In the next section, this traction law is used for the case of shear with negligible normal stress (mode II). A mixed-mode example is analyzed in the coupled behavior section, in which the normal stress as a function of normal displacement has two linear sections (positive slope and then constant slope), and the shear stress as a function of tangential displacement has two linear sections (positive slope and then negative slope). Concluding remarks are presented in the last section.

FORMULATION

Consider Figure 1, in which a tape is peeled from a rigid substrate. The backing that is adhered to the substrate is represented as a semi-infinite, linearly elastic uniform beam. The adhesive is assumed to be linearly elastic for $\tilde{x} < 0$ (shaded region) and to be governed by constant or linearly decreasing traction laws from $\tilde{x} = 0$ to the peel front (dotted region). The free part of the tape to the right of the peel front is replaced by an equivalent resultant bending moment, $\tilde{M}_o$, and an equivalent resultant force with horizontal component, $\tilde{F}_x$, and vertical component, $\tilde{F}_y$, positive as shown. To relate these quantities at the peel front to the applied force or displacement at the free end of the tape, an elastica analysis is sometimes used [19–22]. It allows for large rotations and assumes that the tape is linearly elastic, that its bending moment is proportional to its curvature, and that it is inextensible (although extensibility can be included [23]). The nonlinear equations can be solved numerically in terms of integrals or with the use of a shooting method [24].

The backing has thickness h_b, width w, cross-sectional area $A_b = h_b w$, modulus of elasticity E_b, and moment of inertia $I_b = h_b^3 w/12$. The adhesive has initial thickness h_a. When the adhesive is linearly elastic, it has modulus of elasticity E_a and shear modulus G_a, and the foundation stiffness k is defined as $k = E_a w/h_a$ [25]. The vertical displacement of the centerline of the backing is denoted $\tilde{y}(\tilde{x})$, positive if upward. It is assumed that the applied forces are such that $\tilde{y} > -h_a$.

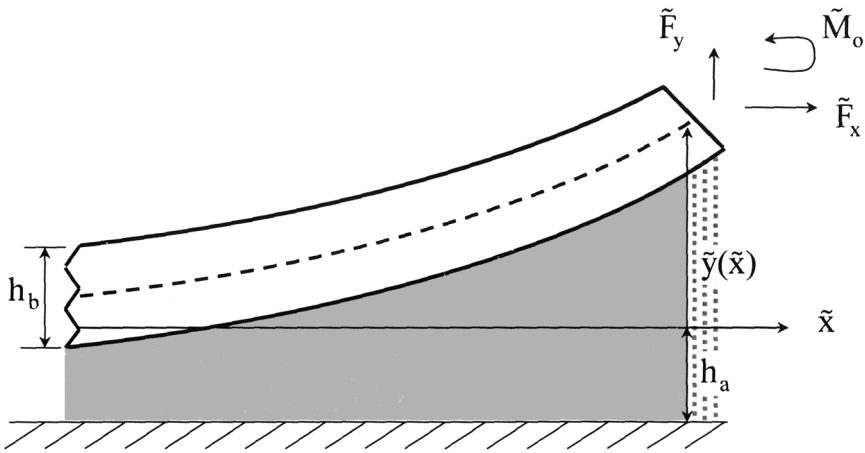

FIGURE 1 Illustration of tape backing and adhesive.

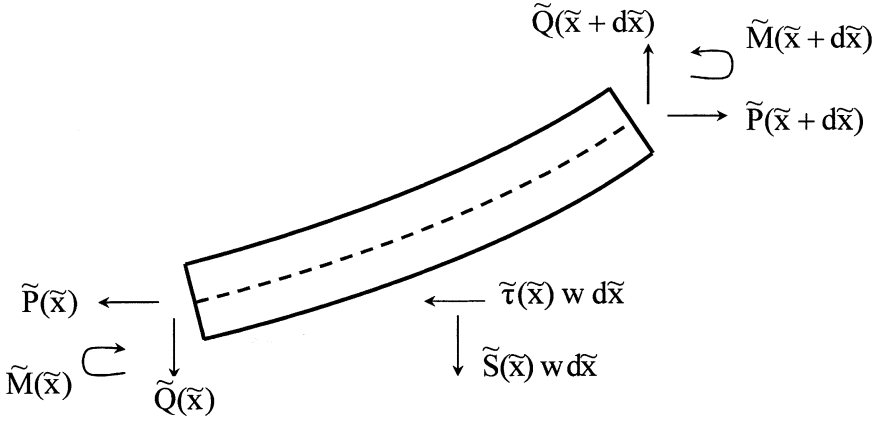

FIGURE 2 Free-body diagram of section of backing with length $d\tilde{x}$.

The slope of the backing is assumed to be small. A free-body diagram of an element of length $d\tilde{x}$ is depicted in Figure 2. At the centerline, the resultant moment is $\tilde{M}$ and the resultant horizontal ("axial") and vertical force components are $\tilde{P}$ and $\tilde{Q}$, respectively. At the interface between the backing and the adhesive, the vertical ("normal") stress is $\tilde{S}$ and the horizontal ("shear") stress is $\tilde{\tau}$. Equilibrium of moments and force components leads to the following equations:

$$\tilde{M}' = \tilde{P}\tilde{y}' - \tilde{Q} + \frac{1}{2} w h_b \tilde{\tau}, \tag{1}$$

$$\tilde{P}' = w\tilde{\tau}, \tag{2}$$

$$\tilde{Q}' = \tilde{S} \tag{3}$$

The moment–curvature relationship is given by

$$\tilde{M} = E_b I_b \tilde{y}''. \tag{4}$$

MODE I

In this section it is assumed that the horizontal forces are negligible, and $\tilde{F}_x$, $\tilde{P}$, and $\tilde{\tau}$ are set equal to zero. From Equations (1), (3), and (4) it follows that

$$E_b I_b \tilde{y}'''' + \tilde{S} = 0. \tag{5}$$

As shown in Figure 3a, $\tilde{y}$ is denoted by $\tilde{y}_1$, $\tilde{y}_2$, and $\tilde{y}_3$, respectively, for $\tilde{x} < 0$ (linearly elastic adhesive), $0 < \tilde{x} < \tilde{r}$ (perfectly plastic

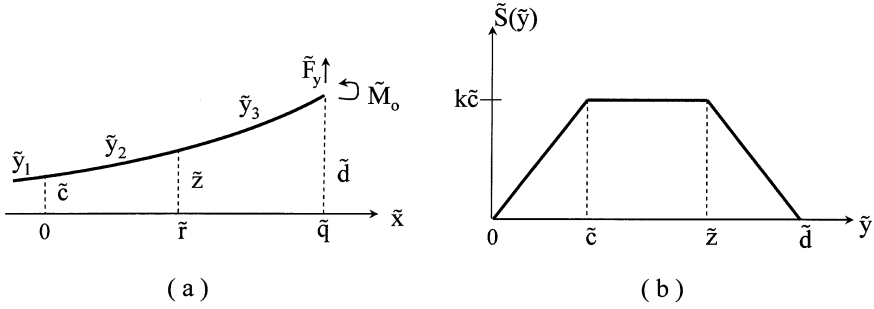

FIGURE 3 Mode I: (a) vertical displacement of backing, (b) normal stress as function of vertical displacement.

adhesive), and $\tilde{r} < \tilde{x} < \tilde{q}$ (damage region). The values of the vertical displacement at $\tilde{x} = 0$, $\tilde{r}$, and $\tilde{q}$ are denoted $\tilde{c}$, $\tilde{z}$, and $\tilde{d}$, respectively. The normal stress $\tilde{S}$ as a function of the vertical displacement is depicted in Figure 3b and is given by

$$\tilde{S}(\tilde{y}) = \begin{cases} k\tilde{y}_1 \text{ if } \tilde{x} < 0, \\ k\tilde{c} \text{ if } 0 < \tilde{x} < \tilde{r}, \\ k\tilde{c}(\tilde{d} - \tilde{y}_3)/(\tilde{d} - \tilde{z}) \text{ if } \tilde{r} < \tilde{x} < \tilde{q} \end{cases} \tag{6}$$

The analysis in this section is carried out in terms of the parameter λ and the nondimensional quantities defined as follows:

$$\begin{gathered} \lambda^4 = \frac{k}{4E_bI_b}, \quad x = \lambda\tilde{x}, \quad y = \lambda\tilde{y}, \quad r = \lambda\tilde{r}, \quad q = \lambda\tilde{q}, \quad c = \lambda\tilde{c}, \\ z = \lambda\tilde{z}, \quad d = \lambda\tilde{d}, \quad S = \frac{\tilde{S}}{4\lambda^3 E_bI_b}, \quad F_y = \frac{\tilde{F}_y}{\lambda^2 E_bI_b}, \\ M_o = \frac{\tilde{M}_o}{\lambda E_bI_b}, \quad \gamma^4 = \frac{4\tilde{c}}{\tilde{d} - \tilde{z}}. \end{gathered} \tag{7}$$

With the use of Equations (5)–(7), the general solutions for the displacement functions have the forms

$$y_1(x) = e^x(a_1 \cos x + a_2 \sin x), \tag{8}$$

$$y_2(x) = a_3 + a_4x + a_5x^2 + a_6x^3 - \frac{c}{6}x^4, \tag{9}$$

$$y_3(x) = d + a_7 \cos \gamma x + a_8 \sin \gamma x + a_9 \cosh \gamma x + a_{10} \sinh \gamma x, \tag{10}$$

where a_j are constant coefficients. The equation for y_1 only has two unknown coefficients due to the finiteness conditions as $x \to -\infty$. Therefore, the boundary value problem involves 10 unknown coefficients,

three displacement values (c, z, and d), and two locations (r and q). Thirteen conditions are available: $y_1 = y_2 = c$ at $x = 0$; $y_2 = y_3 = z$ at $x = r$; $y_3 = d$ at $x = q$; continuity of y', y'', and y''' at $x = 0$ and $x = r$; and at $x = q$, $y_3'' = M_o$ and $y_3''' = -F_y$.

The displacement parameters z and d are written as $z = e_1 c$ and $d = e_2 c$, where $1 < e_1 < e_2$. For given values of F_y, M_o, e_1, and e_2, the 13 conditions are manipulated and reduced to three coupled transcendental equations in the parameters c, r, and q. These equations are solved numerically using the subroutine FindRoot in Mathematica [26]. For the case $F_y = 2$, $M_o = 1$, $e_1 = 1.25$, and $e_2 = 1.75$ (so that $z = 1.46$ and $d = 2.05$), one obtains $c = 1.17$, $r = 0.141$ (the nondimensional length of the plastic region), and $q = 0.390$ (so the nondimensional length of the damage region is 0.249). The displacement is plotted in Figure 4 and the normal stress in the adhesive is shown in Figure 5. The displacement has the usual form for $x < 0$ [1] and continues smoothly upward in the cohesive zone. Compression occurs between approximately $x = -4$ and $x = -1$. In Figure 5, $S = y$ for $x < 0$, $S = c$ for $0 < x < r$, and S(x) decreases almost linearly from c to 0 as x increases from r to q. This is an approximation to the form of the stress determined experimentally in Kaelble and Ho [1], where the slope of the stress did not exhibit discontinuities.

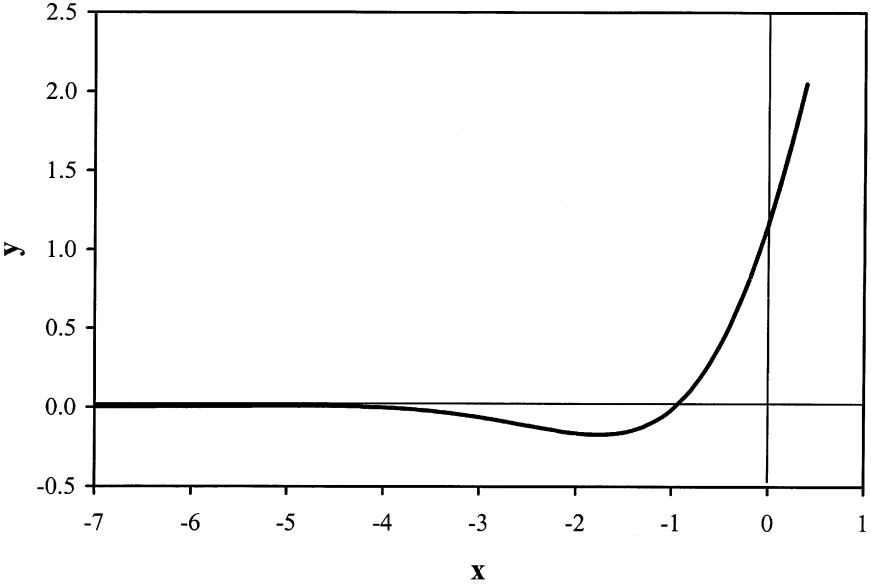

FIGURE 4 Vertical displacement for mode I example.

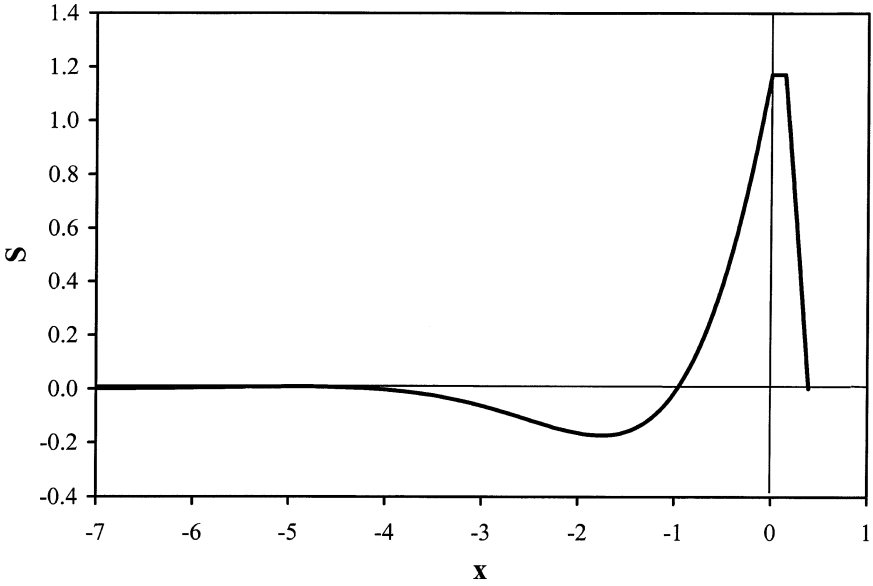

FIGURE 5 Normal stress for mode I example.

For this example, in order to compare the displacement in Figure 4 with that for the case with no cohesive zone, Equation (8) is applied for the entire region $x < 0.390$. Application of the boundary conditions $y''(0.390) = 1$ and $y'''(0.390) = -2$ leads to $a_1 = 0.811$ and $a_2 = 0.699$. The shape is similar to that in Figure 4, but the displacements at $x = 0$, 0.141, and 0.390 for this model are 0.811, 1.04, and 1.50, respectively, which are smaller than the values 1.17, 1.46, and 2.05 when the cohesive zone is included.

MODE II

Now it is assumed that $\tilde{F}_y$, $\tilde{M}_o$, $\tilde{Q}$, $\tilde{M}$, and $\tilde{S}$ are negligible, and they are set equal to zero, so the focus is on the shear stress, $\tilde{\tau}$, caused by the applied horizontal force, $\tilde{F}_x$. The horizontal displacement of a bottom fiber of the backing is denoted $\tilde{u}(\tilde{x})$, positive in the $\tilde{x}$ direction. The constitutive law for extension of the backing is assumed to be

$$\tilde{P} = wh_bE_b\tilde{u}'. \tag{11}$$

Consider Figure 6. The cohesive zone for shear assumed here is similar to what it was for tension in the preceding section, and subscripts 1, 2, and 3 denote quantities in the elastic, plastic, and damage

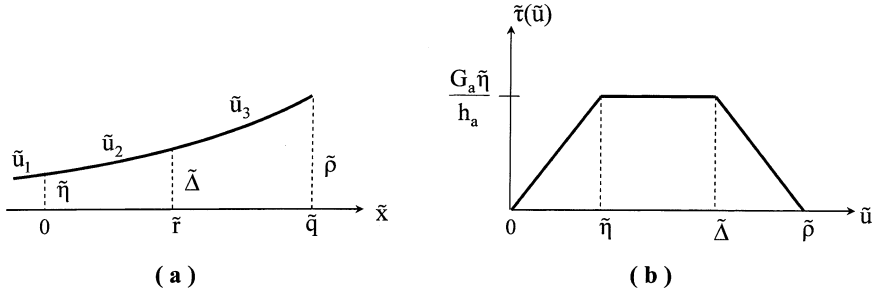

FIGURE 6 Mode II: (a) horizontal displacement at bottom of backing, (b) shear stress as function of horizontal displacement.

regions, respectively. The values of $\tilde{u}(\tilde{x})$ at $\tilde{x} = 0$, $\tilde{r}$, and $\tilde{q}$ are denoted $\tilde{\eta}$, $\tilde{\Delta}$, and $\tilde{\rho}$, respectively.

The parameters α and s are defined by the following relations:

$$\alpha^2 = \frac{G_a}{h_a h_b E_b}, \qquad s^2 = \frac{\tilde{\eta}}{(\tilde{\rho} - \tilde{\Delta})}. \tag{12}$$

Based on Figure 6 and Equations (2) and (11), for the elastic region ($\tilde{x} < 0$) the shear stress, $\tilde{\tau}_1$, at the bottom of the backing and the axial force, $\tilde{P}_1$, satisfy the equations

$$\tilde{\tau}_1 = G_a \frac{\tilde{u}_1}{h_a}, \qquad \tilde{P}_1'' - \alpha^2 \tilde{P}_1 = 0. \tag{13}$$

In the plastic region ($0 < \tilde{x} < \tilde{r}$),

$$\tilde{\tau}_2 = \frac{G_a \tilde{\eta}}{h_a}, \qquad \tilde{P}_2' = \frac{G_a w \tilde{\eta}}{h_a}. \tag{14}$$

Finally, in the damage region ($\tilde{r} < \tilde{x} < \tilde{q}$),

$$\tilde{\tau}_3 = \frac{G_a \tilde{\eta}(\tilde{\rho} - \tilde{u}_3)}{h_a(\tilde{\rho} - \tilde{\Delta})}, \qquad \tilde{P}_2'' + s^2 \alpha^2 \tilde{P}_3 = 0. \tag{15}$$

The following nondimensional quantities are defined for this mode-II analysis:

$$\begin{gathered} \bar{x} = \alpha \tilde{x}, \quad \bar{r} = \alpha \tilde{r}, \quad \bar{q} = \alpha \tilde{q}, \quad u = \frac{\tilde{u}}{\tilde{\eta}}, \quad \Delta = \frac{\tilde{\Delta}}{\tilde{\eta}}, \quad \rho = \frac{\tilde{\rho}}{\tilde{\eta}}, \\ \bar{\tau} = \frac{h_a \tilde{\tau}}{G_a \tilde{\eta}}, \quad \bar{P} = \frac{\alpha h_a \tilde{P}}{G_a \tilde{\eta} w}, \quad \bar{F}_x = \frac{\alpha h_a \tilde{F}_x}{G_a \tilde{\eta} w}. \end{gathered} \tag{16}$$

It is noted that the nondimensional quantities $\bar{x}$, $\bar{r}$, and $\bar{q}$ are not the same as x, y, and r used in the preceding section.

From Equations (13)–(15) in nondimensional form, general solutions for $\bar{P}_1$, $\bar{P}_2$, and $\bar{P}_3$ can be written, and general solutions for $\bar{\tau}_j$ and u_j can be obtained from $\bar{\tau}_j = \bar{P}_j'$ and $u_j' = \bar{P}_j$ ($j = 1,2,3$) based on Equations (2) and (11). The unknown coefficients can be determined with the use of the following conditions: finiteness as $\bar{x} \to -\infty$; $u_1 = u_2 = 1$ at $\bar{x} = 0$; $u_2 = u_3 = \Delta$ at $\bar{x} = \bar{r}$; $u_3 = \rho$ at $\bar{x} = \bar{q}$; continuity of u, $\bar{\tau}$, and $\bar{P}$ at $\bar{x} = 0$ and $\bar{x} = \bar{r}$; and, at $\bar{x} = \bar{q}$, $\bar{\tau} = 0$ and $\bar{P} = \bar{F}_x$.

The solution for $u_j(\bar{x})$, $j = 1, 2, 3$, is

$$u_1(\bar{x}) = e^{\bar{x}}, \quad u_2(\bar{x}) = 1 + \bar{x} + \frac{1}{2}\bar{x}^2,$$
$$u_3(\bar{x}) = \rho - \frac{(1+\bar{r})}{s}\sin[s(\bar{r} - \bar{x})] - \frac{1}{s^2}\cos[s(\bar{r} - \bar{x})]. \tag{17}$$

Then $\bar{P}_j = u_j'$ and $\bar{\tau}_j = u_j''$. From the required conditions, it is found that the following equations must be satisfied:

$$\bar{F}_x = \sqrt{\rho + \Delta - 1}, \qquad \bar{r} = \sqrt{2\Delta - 1} - 1,$$
$$\bar{q} = \bar{r} + \frac{1}{s}\text{Arc tan}\left[\frac{1}{s(1+\bar{r})}\right]. \tag{18}$$

One can set Δ and ρ, and obtain $\bar{F}_x$, $\bar{r}$, and $\bar{q}$ from Equation (18). As a numerical example, suppose that $\Delta = 1.25$ and $\rho = 1.75$; then $\bar{r} = 0.225$, $\bar{q} = 0.595$, and $\bar{F}_x = \sqrt{2}$. The corresponding functions $u(\bar{x})$, $\bar{P}(\bar{x})$, and $\bar{\tau}(\bar{x})$ are plotted in Figures 7, 8, and 9, respectively. The curve of the tensile axial force $\bar{P}(\bar{x})$ is smooth and has zero slope at the peel front. The shear stress $\bar{\tau}(\bar{x})$ has the standard exponential solution for $\bar{x} < 0$, is constant for $0 < \bar{x} < \bar{r}$, and is almost linear from unity to zero as $\bar{x}$ increases from $\bar{r}$ to $\bar{q}$.

The results for this example can be compared with the classical case without a cohesive zone. In that case, the first equation in Equation (17) governs for $\bar{x} < 0.595$, and $u(0.225)$ is 1.25 again, but $u(0.595)$ is 1.81, which is higher than the value 1.75 with the cohesive zone.

COUPLED BEHAVIOR (MIXED MODES)

Finally, consider the case in which neither normal nor shear stresses are negligible. Equations (1)–(4) are applicable. If Equation (1) is differentiated and Equations (3) and (4) are utilized, one obtains

$$E_b I_b \tilde{y}'''' + \tilde{S} - \frac{1}{2} w h_b \tilde{\tau}' = (\tilde{P}\tilde{y}')'. \tag{19}$$

The term on the right-hand side of Equation (19) is nonlinear when $\tilde{P}$ and $\tilde{y}$ are variables, and it is neglected. This term was not included in

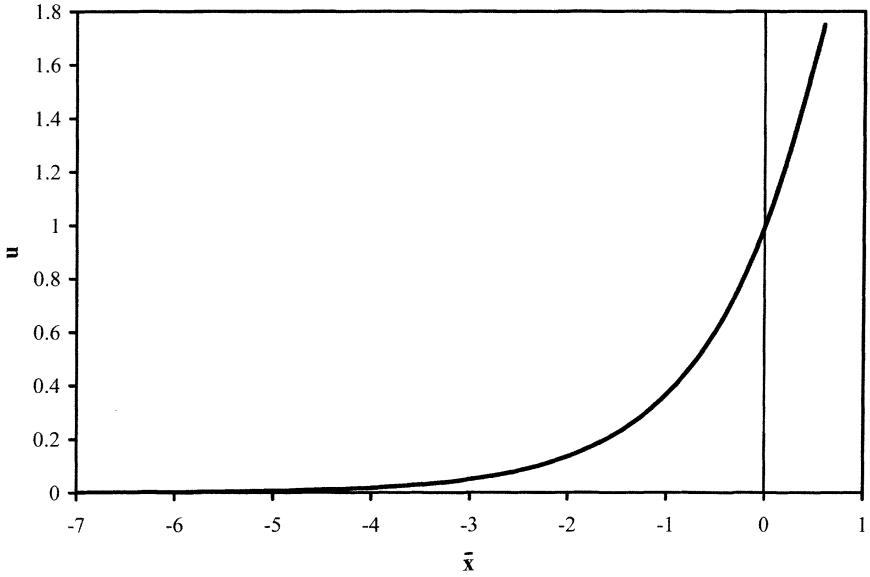

FIGURE 7 Horizontal displacement for mode II example.

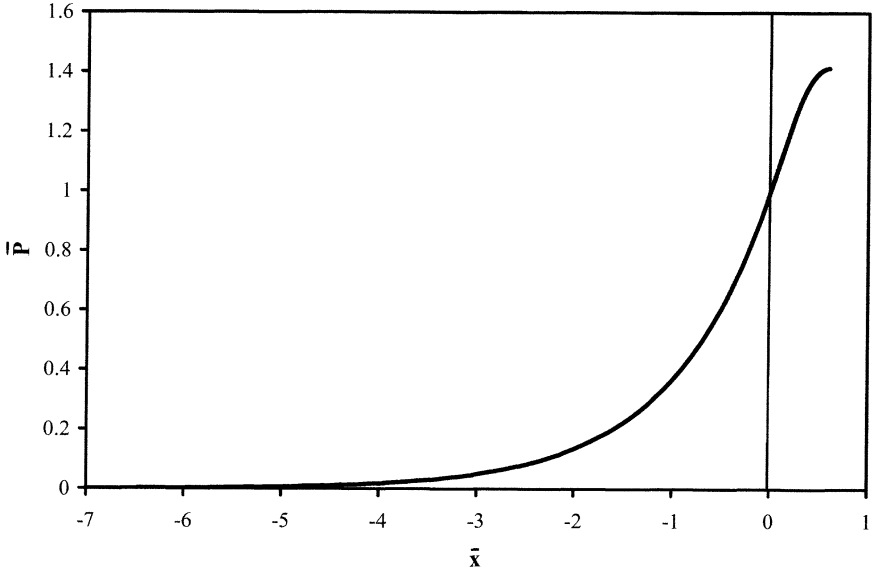

FIGURE 8 Axial force for mode II example.

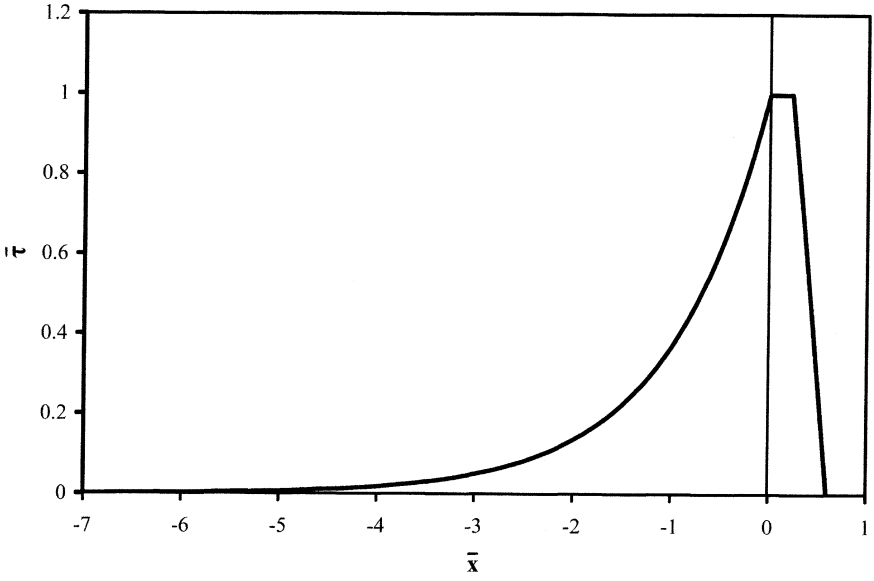

FIGURE 9 Shear stress for mode II example.

the derivations in Goland and Reissner [27], Sneddon [28], and Bigwood and Crocombe [29], and in Cornell [30] it was dropped since it provides a "second-order effect" when the displacements are small. The magnitude of this term will be examined later for an example.

Due to bending and extension of the centerline of the backing, the horizontal displacement, $\tilde{u}(\tilde{x})$, of a bottom fiber of the backing satisfies [27,28]

$$\tilde{u}' = \frac{1}{2} h_b \tilde{y}'' + \frac{\tilde{P}}{w h_b E_b}. \tag{20}$$

Consider the traction laws shown in Figure 10. A similar law for the normal stress was considered in Williams and Hadavinia [12] and Yamada [15]. Subscript 1 denotes quantities for $\tilde{x} < 0$ and subscript 2 for $0 < \tilde{x} < \tilde{r}$ in which the normal stress is constant and the shear stress decreases linearly to zero as a function of the horizontal displacement, $\tilde{u}$, so that the required shear stress condition at the peel front is satisfied. The normal stress, $\tilde{S}$, is given by the first two expressions in Equation (6), the shear stress, $\tilde{\tau}_1$, is given in Equation (13), and the shear stress, $\tilde{\tau}_2$, is

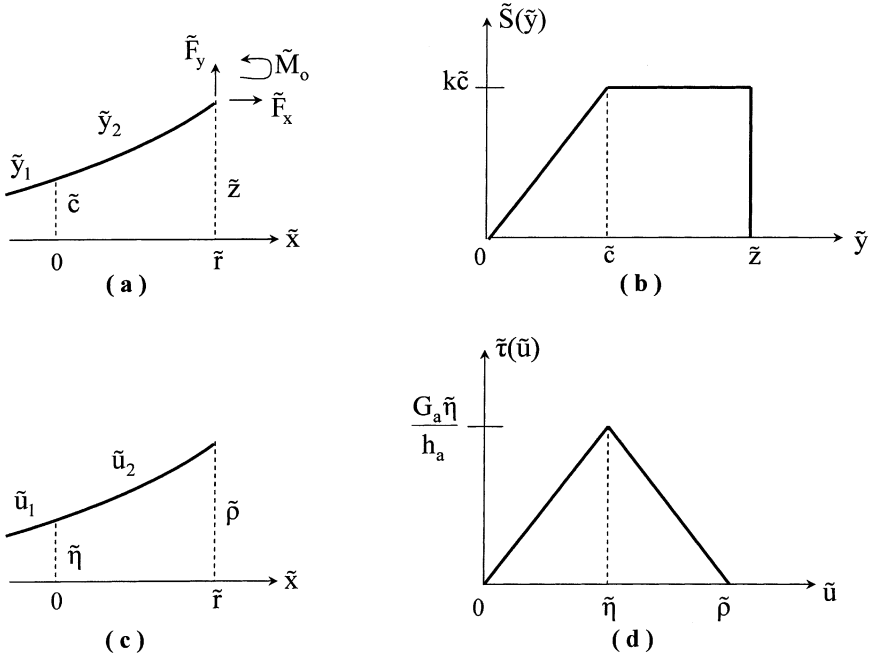

FIGURE 10 Coupled modes: (a) vertical displacement of backing; (b) normal stress as function of vertical displacement; (c) horizontal displacement at bottom of backing; (d) shear stress as function of horizontal displacement.

$$\tilde{\tau}_2 = \frac{G_a\tilde{\eta}(\tilde{\rho} - \tilde{u}_2)}{h_a(\tilde{\rho} - \tilde{\eta})}. \tag{21}$$

The justification for different traction–separation relationships for normal and shear stresses is discussed in Thouless and Yang [9].

Using these stresses along with Equation (2), Equation (19) without its right-hand side, and Equation (20), the governing equations for $\tilde{x} < 0$ can be written in terms of $\tilde{y}_1(\tilde{x})$ and $\tilde{P}_1(\tilde{x})$ as

$$E_b I_b \tilde{y}_1'''' - k\tilde{y}_1 - \frac{1}{2}h_b\tilde{P}_1'' = 0, \tag{22}$$

$$\frac{1}{2}h_b\tilde{y}_1'' - \frac{h_a}{wG_a}\tilde{P}_1'' + \frac{\tilde{P}_1}{wh_bE_b} = 0. \tag{23}$$

These are special cases of equations used in Bigwood and Crocombe [30]. For $0 < \tilde{x} < \tilde{r}$, the governing equations in terms of $\tilde{y}_2(\tilde{x})$ and $\tilde{P}_2(\tilde{x})$ are

$$E_b I_b \tilde{y}_2'''' - \frac{1}{2} h_b \tilde{P}_2'' = -k\tilde{c}, \tag{24}$$

$$\frac{1}{2} h_b \tilde{y}_2'' + \frac{h_a(\tilde{\rho} - \tilde{\eta})}{w G_a \tilde{\eta}} \tilde{P}_2'' + \frac{\tilde{P}_2}{w h_b E_b} = 0. \tag{25}$$

The analysis is carried out in nondimensional terms. The quantities λ, x, y, r, c, z, S, F_y, and M_o are defined in Equation (7), and new variables used here are

$$\tau = \frac{w h_b \tilde{\tau}}{2\lambda^2 E_b I_b}, \qquad P = \frac{h_b \tilde{P}}{2\lambda E_b I_b}, \qquad F_x = \frac{h_b \tilde{F}_x}{2\lambda E_b I_b}. \tag{26}$$

Equations (22)–(25) then take the following form:

$$y_1'''' + 4y_1 - P_1'' = 0, \tag{27}$$

$$3\xi^2 y_1'' - P_1'' + \xi^2 P_1 = 0, \tag{28}$$

$$y_2'''' - P_2'' = -4c, \tag{29}$$

$$3\Omega^2 y_2'' + 4P_2'' + \Omega^2 P_2 = 0, \tag{30}$$

where

$$\xi^2 = \frac{\alpha^2}{\lambda^2}, \qquad \Omega^2 = \frac{4\xi^2 \tilde{\eta}}{(\tilde{\rho} - \tilde{\eta})}, \tag{31}$$

and α is defined in Equation (12).

For $x < 0$, the general solution of Equations (27) and (28) has the form

$$y_1(x) = \mathrm{Re}\left\{\sum_{j=1}^{6} a_j e^{\Lambda_j x}\right\}, \quad P_1(x) = \mathrm{Re}\left\{\sum_{j=1}^{6} a_j \left(\Lambda_j^2 + \frac{4}{\Lambda_j^2}\right) e^{\Lambda_j x}\right\}, \tag{32}$$

where a_j are constants and Λ_j are the roots of the following cubic equation in Λ^2:

$$\Lambda^6 - 4\xi^2 \Lambda^4 + 4\Lambda^2 - 4\xi^2 = 0. \tag{33}$$

Some of the a_j and Λ_j are complex. For $0 < x < r$, the general solution of Equations (29) and (30) can be written as

$$\begin{aligned} y_2(x) &= b_1 + b_2 x + b_3 x^2 + b_4 x^3 - \frac{c x^4}{24} + b_5 \sin \Omega x + b_6 \cos \Omega x, \\ P_2(x) &= -6b_3 - 18 b_4 x + \frac{3cx^2}{2} - \frac{12c}{\Omega^2} - \Omega^2 b_5 \sin \Omega x - \Omega^2 b_6 \cos \Omega x, \end{aligned} \tag{34}$$

where b_j are constants.

In order to determine the unknown coefficients, the finiteness conditions as $x \to -\infty$ are applied, as well as conditions at $x = 0$ and r. At $x = 0$, $y_1 = y_2 = c$, and the quantities y', y'', y''', P, and P' are continuous. At $x = r$, the boundary conditions are $P_2 = F_x$, $y_2'' = M_o$, and $y_2''' = -F_y$.

For a numerical example, let $\xi^2 = 0.001$, $r = 0.5$, $F_x = 0.2$, $F_y = 0.4$, and $M_o = 0$. The resulting plots for the vertical displacement y(x), normal stress S(x), axial force P(x) in the backing, and shear stress $\tau(x)$ at the bottom of the backing are presented in Figures 11–14, respectively. The horizontal scales in Figures 13 and 14 are much different from those in Figures 11 and 12. At $x = 0$, $y = S = 0.129$, $P = 0.198$, and $\tau = 0.00684$. At the peel front $x = 0.5$, naturally S is the same as at $x = 0$, and $y = 0.239$, $P = F_x = 0.2$, and $\tau = 0$.

If this example were analyzed without a cohesive zone, Equations (27) and (28) would be applied for $x < r$ and the solution would satisfy the boundary conditions at $x = r$. The resulting deflection can be written as

$$y(x) = 4.91 \times 10^{-5} e^{0.0316x} + e^{-x}(0.107 \cos x + 0.200 \sin x). \qquad (35)$$

At $x = 0$ for this solution, $y = S = 0.107$, $P = 0.197$, and $\tau = 0.00670$, and at the peel front $x = 0.5$, $y = S = 0.200$, $P = 0.2$, and $\tau = 0.00691$.

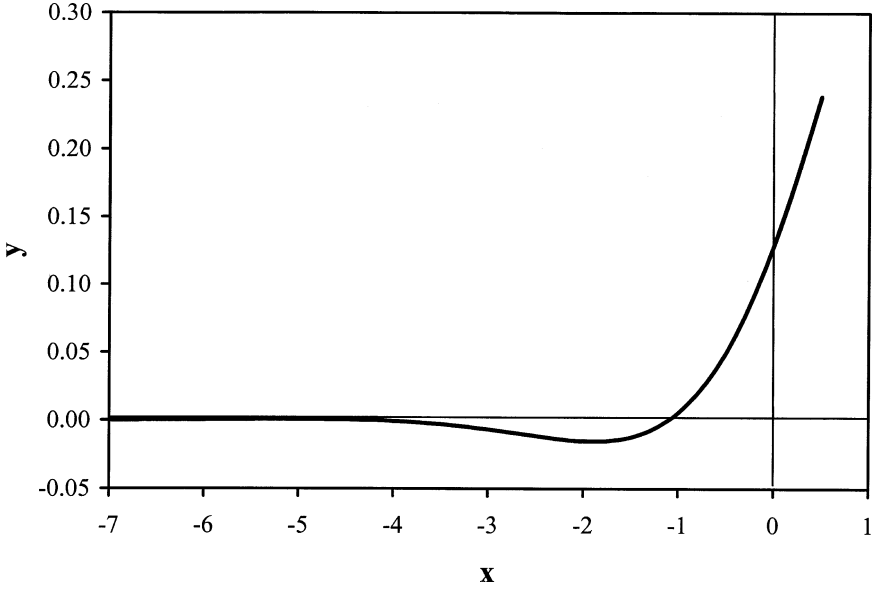

FIGURE 11 Vertical displacement for mixed-mode example.

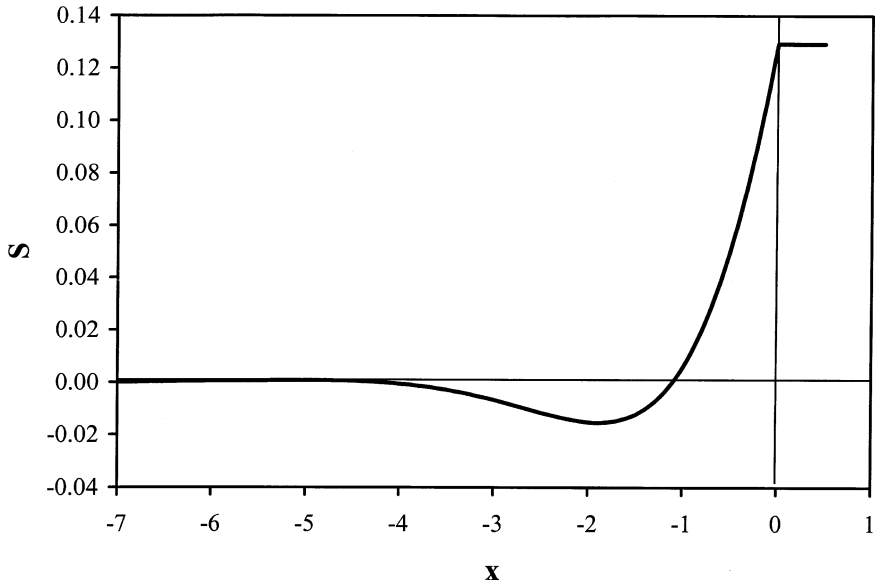

FIGURE 12 Normal stress for mixed-mode example.

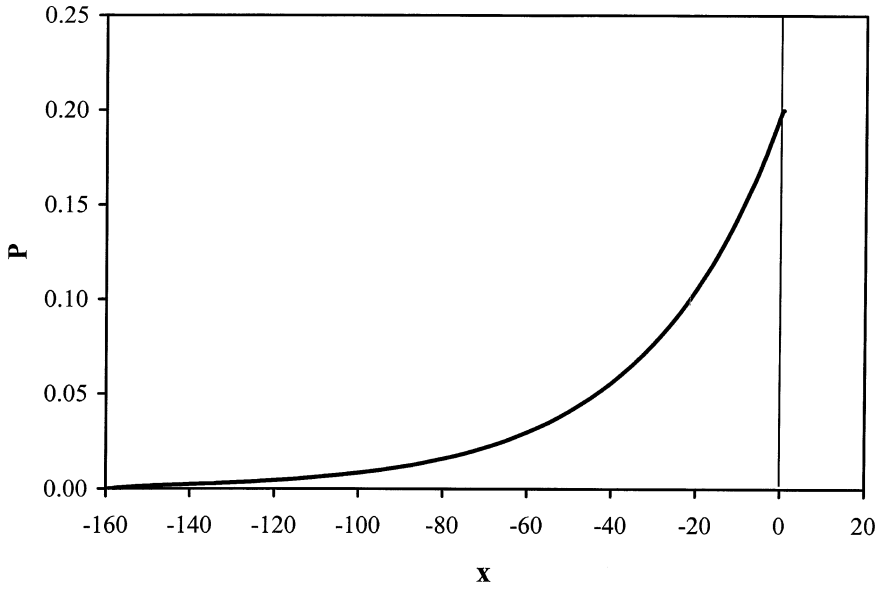

FIGURE 13 Axial force for mixed-mode example.

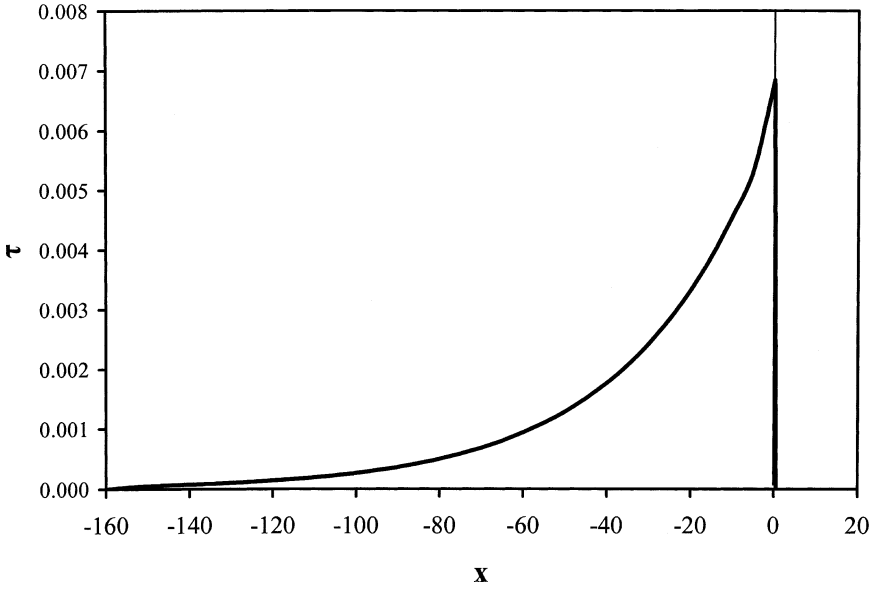

FIGURE 14 Shear stress for mixed-mode example.

Finally, it is desirable to get an idea of the size of the term on the right-hand side of Equation (19), which was neglected in order to obtain linear equations with analytical solutions. In the nondimensional Equations (27) and (29), it would add the expression $2(P_j y_j')'/(\lambda h_b)$ to the right-hand sides ($j = 1,2$, respectively), which can be compared with the other terms. In the numerical example, the quantities y'''', y, P'', and $(Py')'$ have the respective values -0.52, 0.13, 0.0006, and 0.03 at $x = 0$, for instance. Whether or not the neglected term is small compared with the other three terms depends on the nondimensional product λh_b, which is equal to $[3h_b E_a/(h_a E_b)]^{1/4}$. It follows that the term will be negligible if the product of h_b/h_a and E_a/E_b is sufficiently large. If it is not, a nonlinear analysis would be needed.

CONCLUDING REMARKS

Several objectives have motivated this study. One has been to obtain solutions that satisfy the condition of zero shear stress at the peel front, as well as solutions in which the normal stress in the adhesive reduces to zero at the peel front (to model the behavior when fibrillation causes this to occur). Also, it was desired to derive analytical solutions for the displacements and stresses, for which the coefficients

could be computed using boundary and transition conditions. Hence, formulations leading to piecewise-linear differential equations with constant coefficients were considered. This led to the model of the tape backing in the adhered region as a linearly elastic beam with small slopes, and traction–separation laws for the normal and shear stresses consisting of linear sections. The free part of the tape, beyond the peel front, does not need to be linearly elastic or to have small slopes, and it was represented by equivalent force and bending moment resultants at the peel front.

Three formulations were presented. In the first, the shear stress was negligible (mode I). As an example, a trapezoidal cohesive zone was assumed for the normal stress in the adhesive. In the second formulation, the normal stress was negligible (mode II), and a similar cohesive zone was assumed for the shear stress at the interface of the backing and the adhesive (this model may be more useful for lap joints than for peel tests). Finally, a mixed-mode model was considered, involving coupled normal and shear stresses. In the example, the normal stress was perfectly plastic near the peel front, while the shear stress decreased to zero.

Due to the kinks in the traction-separation laws, the resulting plots of normal and shear stress *versus* position along the tape demonstrate unrealistic kinks (although the relationships for displacements and axial force in the backing are smooth). However, the results approximate those that would be obtained if similar traction laws without sharp corners would be assumed.

For the mixed-mode model, it was assumed that the shear stress was zero at the peel front. A failure criterion based on the fracture energy could be considered, with the shear stress not reaching zero. The components G_I and G_{II} of the fracture energy are defined by

$$G_I = \int_0^{\tilde{y}} S(\tilde{y})d\tilde{y}, \qquad G_{II} = \int_0^{\tilde{u}} \tilde{\tau}(\tilde{u})d\tilde{u}, \tag{36}$$

and the failure criterion can be chosen as [9, 31]

$$\frac{G_I}{\Gamma_{Io}} + \frac{G_{II}}{\Gamma_{IIo}} = 1, \tag{37}$$

where Γ_{Io} and Γ_{IIo} are the total areas under the mode I and mode II traction–separation laws, respectively. For the traction laws in Figure 10, Equation (36) becomes

$$\frac{2y - c}{2z - c} + \frac{2\rho u - \rho - u^2}{\rho(\rho - 1)} = 1 \tag{38}$$

where the nondimensional quantities are defined in Equations (7) and (16). As the applied forces are increased, peeling is assumed to occur when the displacements y and u satisfy Equation (37).

In the global context of the displacements and stresses, the local behavior near the peel front may not cause significant changes. However, in some cases it is of interest, and a cohesive zone can be an effective means to model such behavior. Analytical solutions, even if based on some restrictive assumptions, can be useful in uncovering some of the features of the local displacements and stresses, and in some cases it is important to include the mixed-mode coupled behavior of the normal and shear stresses.

REFERENCES

[1] Kaelble, D. H., and Ho, C. L., *Trans. Soc. Rheology* **18**, 219–235 (1974).
[2] Kaelble, D. H., *Trans. Soc. Rheology* **4**, 45–73 (1960).
[3] Wang, C. H., Heller, M., and Rose, L. R. F., *J. Strain Analysis* **33**, 331–346 (1998).
[4] Allmann, D. J., *Quarterly J. Mechanics Appl. Math.* **30**, 415–436 (1977).
[5] Chen, D., and Cheng, S., *J. Appl. Mech.* **50**, 109–115 (1983).
[6] Adams, R. D., and Mallick, V., *J. Adhesion* **38**, 199–217 (1992).
[7] Yang, Q. D., Thouless, M. D., and Ward, S. M., *J. Mech. Phys. Solids* **47**, 1337–1353 (1999).
[8] Yang, Q. D., Thouless, M. D., and Ward, S. M., *Int. J. Solids Structures* **38**, 3251–3262 (2001).
[9] Thouless, M. D., and Yang, Q. D., In: *The Mechanics of Adhesion*, D. A. Dillard and A. V. Pocius, Eds. (Elsevier, Amsterdam, 2002), pp. 235–271.
[10] Wei, Y., and Hutchinson, J. W., *Int. J. Fracture* **93**, 315–333 (1998).
[11] Yang, Q. D., Thouless, M. D., and Ward, S. M., *J. Adhesion* **72**, 115–132 (2000).
[12] Williams, J. G., and Hadavinia, H., *J. Mech. Phys. Solids* **50**, 809–825 (2002).
[13] Zosel, A., *J. Adhesion* **30**, 135–149 (1989).
[14] Creton, C., and Fabre, P., In: *The Mechanics of Adhesion*, D. A. Dillard and A. V. Pocius, Eds. (Elsevier, Amsterdam, 2002), pp. 535–575.
[15] Yamada, S. E., *Eng. Fracture Mech.* **27**, 315–328 (1987).
[16] Georgiou, I., Hadavinia, H., Ivankovic, A., Kinloch, A. J., Tropsa, V., and Williams, J. G., *J. Adhesion* **79**, 239–265 (2003).
[17] Rahulkumar, P., Jagota, A., Bennison, S. J., and Saigal, S., *Int. J. Solids Structures* **37**, 1873–1897 (2000).
[18] Cotterell, B., Williams, G., Hutchinson, J., and Thouless, M., *Int. J. Fracture* **119**, L55–L59 (2003).
[19] Kendall, K., *J. Adhesion* **5**, 105–117 (1973).
[20] Thouless, M. D., and Jensen, H. M., *J. Adhesion* **38**, 185–197 (1992).
[21] Kogan, L., Hui, C. Y., Kramer, E. J., and Wallace, E., Jr., *J. Adhesion Sci. Technol.* **12**, 71–94 (1998).
[22] Lin, Y. Y., Hui, C. Y., and Wang, Y. C., *J. Appl. Polymer Sci. B* **40**, 2277–2291 (2002).
[23] Britvec, S. J., *The Stability of Elastic Systems* (Pergamon Press, New York, 1973).
[24] Plaut, R. H., Suherman, S., Dillard, D. A., Williams, B. E., and Watson, L. T., *Int. J. Solids Structures* **36**, 1209–1229 (1999).

[25] Dillard, D. A., In: *The Mechanics of Adhesion*, D. A. Dillard and A. V. Pocius, Eds. (Elsevier, Amsterdam, 2002), pp. 1–44.
[26] Wolfram, S., *The Mathematica Book*, 3rd ed. (Cambridge University Press, Cambridge, UK, 1996).
[27] Goland, M., and Reissner, E., *J. Appl. Mech.* **11**, A17–A27 (1944).
[28] Sneddon, I. N., In: *Adhesion*, D. D. Eley, Ed. (Oxford University Press, Oxford, 1961), pp. 207–253.
[29] Bigwood, D. A., and Crocombe, A. D., *Int. J. Adhesion Adhesives* **9**, 229–242 (1989).
[30] Cornell, R. W., *J. Appl. Mech.* **20**, 355–364 (1953).
[31] Yang, Q. D., and Thouless, M. D., *Int. J. Fracture* **110**, 175–187 (2001).